

## Contents

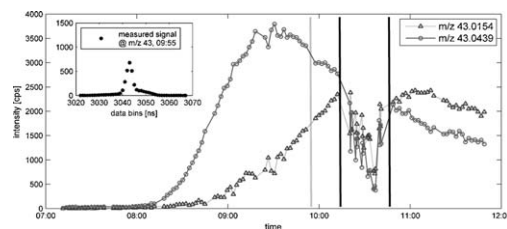
### Regular articles

1–8

#### Enhanced spectral analysis of C-TOF Aerosol Mass Spectrometer data: Iterative residual analysis and cumulative peak fitting

Markus Müller, Christian George, Barbara D'Anna

► Improved peak analysis due to cumulative peak fitting and iterative residual analysis. ► Simulations of the separation power of the algorithm using a synthetic double-peak system. ► Demonstrations of limits for peak fitting for C-TOF AMS, HR-TOF AMS and PTR-TOF. ► Successful separation of isobars using a C-TOF AMS.

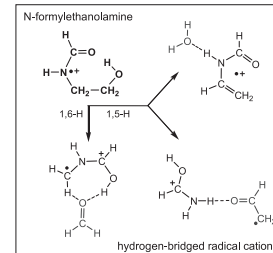


9–26

#### The dissociation chemistry of low-energy *N*-formylethanolamine ions: Hydrogen-bridged radical cations as key intermediates

Karl J. Jobst, Richard D. Bowen, Johan K. Terlouw

► Metastable *N*-formylethanolamine ions lose H<sub>2</sub>O, CH<sub>2</sub>O and CH<sub>2</sub> = CHO•. ► Hydrogen-bridged radical cations are predicted by theory to be key intermediates. ► Part of the C<sub>2</sub>H<sub>3</sub>O• loss may involve CH<sub>3</sub>CO•, generated by quid-pro-quo catalysis.

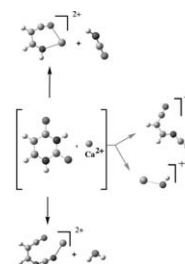


27–36

#### Unimolecular reactivity upon collision of uracil–Ca<sup>2+</sup> complexes in the gas phase: Comparison with uracil–M<sup>+</sup> (M = H, alkali metals) and uracil–M<sup>2+</sup> (M = Cu, Pb) systems

Cristina Trujillo, Al Mokhtar Lamsabhi, Otilia Mó, Manuel Yáñez, Jean-Yves Salpin

► Interaction of Ca<sup>2+</sup> ions with uracil studied by MS/MS and DFT calculations. ► Use of labeled uracils for more detailed information. ► Potential energy surfaces of the various fragmentations explored. ► Comparison with the reactivity induced by other monocations or dications.

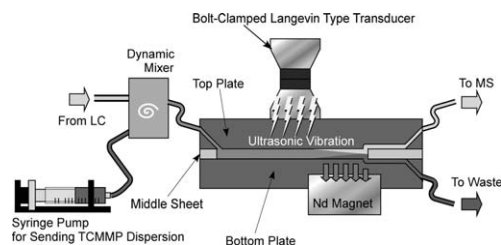


## 37–43

### Demonstration of on-line desalination for LC–MS using phosphate adsorption onto TiO<sub>2</sub>-coated magnetic microparticles within a microchannel

Yoshitake Akiyama, Yutaka Takahashi, Issei Akutagawa, Akira Ono, Keisuke Morishima, Kazuhiro Chiba

► The desalination interface device (DID) for LC–MS was developed. ► Phosphate was adsorbed onto TiO<sub>2</sub>-coated magnetic microparticles. ► The S/N ratio in the mass spectra of reserpine was increased 5.3-fold by LC–DID–MS.

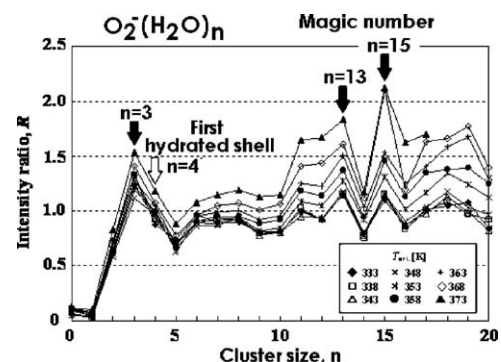


## 44–50

### Temperature dependence of magic number and first hydrated shell of various core water cluster ions Y<sup>-</sup>(H<sub>2</sub>O)<sub>n</sub> (Y = O<sub>2</sub>, HO, NO<sub>x</sub>, CO<sub>x</sub>) in atmospheric pressure negative corona discharge mass spectrometry

Kanako Sekimoto, Kei Kikuchi, Mitsuo Takayama

► Water clusters Y<sup>-</sup>(H<sub>2</sub>O)<sub>n</sub> (Y = O<sub>2</sub>, HO, HO<sub>2</sub>, NO<sub>2</sub>, NO<sub>3</sub>, NO<sub>3</sub>(HNO<sub>3</sub>)<sub>2</sub>, CO<sub>3</sub>, HCO<sub>4</sub>; n = 0–30) were produced by a corona discharge device. ► The magic number and first hydrated shell in the cluster ions Y<sup>-</sup>(H<sub>2</sub>O)<sub>n</sub> were observed. ► The reliability of the magic number and first hydrated shell was confirmed by varying orifice temperature.

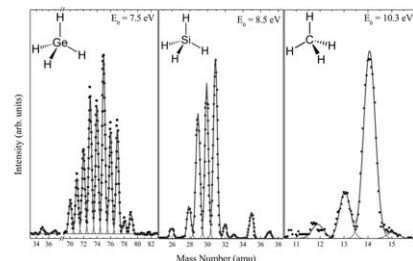


## 51–56

### Negative ion formation through dissociative electron attachment to GeH<sub>4</sub>: Comparative studies with CH<sub>4</sub> and SiH<sub>4</sub>

M. Hoshino, Š. Matejčík, Y. Nunes, F. Ferreira da Silva, P. Limão-Vieira, H. Tanaka

► Negative ion formation by low-energy electron impact to germane (GeH<sub>4</sub>) has been performed in an electron energy region from 6 to 11 eV with an energy resolution of ~500 meV. ► Anion efficiency curves of four anions have been measured. ► Fragmentation into these negative ions is attributed to resonant dissociative electron attachment processes.

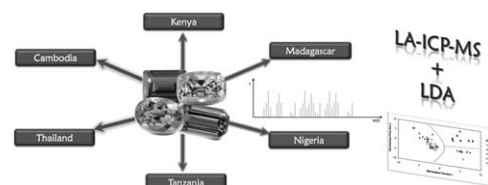


## 57–62

### Geographical origin classification of gem corundum using elemental fingerprint analysis by laser ablation inductively coupled plasma mass spectrometry

Pornwilard M.-M., Rak Hansawek, Juwadee Shiowatana, Atitaya Siripinyanond

► The LDA mapping can separate rubies between South East Asia and African countries and blue sapphires from Madagascar and Nigeria. ► B, Si, Zn, Ga, Sn, V, Mg, Ti, Cr and Fe were effective for classification of blue sapphires from Madagascar and Nigeria. ► The ratio of Si and B concentrations were able to distinguish the Cambodian and the Thai gem corundum.

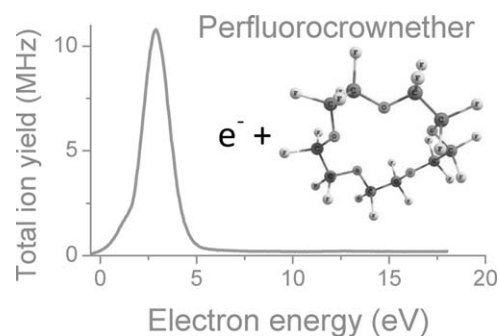


## 63–69

**Strong fragmentation processes driven by low energy electron attachment to various small perfluoroether molecules**

C. Mitterdorfer, A. Edtbauer, S. Karolczak, J. Postler, D. Gschliesser, S. Denifl, E. Illenberger, P. Scheier

► Studied perfluoroether are sensitive towards subexcitation electrons. ► Fragment anions are formed by loss of neutral  $\text{CF}_2$ ,  $\text{CF}_3$  and  $\text{CF}_2\text{OCF}_3$  units. ► Electrons contribute to degradation of perfluoropolyether films on hard discs.

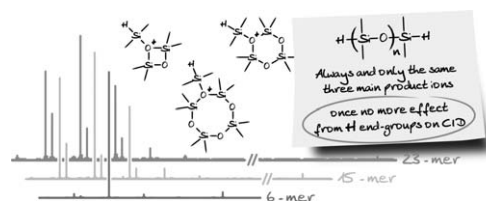


## 70–76

**Dissociation characteristics of  $\alpha,\omega$ -dihydride poly(dimethylsiloxane) ammonium adducts generated by electrospray ionization**

Thierry Fouquet, Stéphane Humbel, Laurence Charles

► CID of ammonium adducts of hydride-terminated PDMS has been established. ► The same three main ions are always produced, regardless of the precursor ion size. ► Reactivity of hydride end-groups is emphasized for smallest oligomers. ► Perfect similarity is obtained for MS/MS spectra of highest congeners.

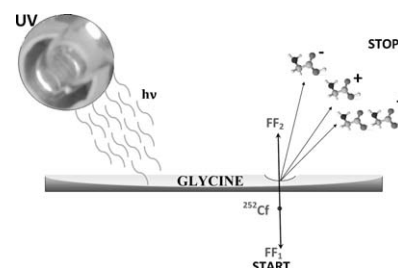


## 77–81

**Photostability of amino acids to Lyman  $\alpha$  radiation: Glycine**

A.M. Ferreira-Rodrigues, M.G.P. Homem, A. Naves de Brito, C.R. Ponciano, E.F. da Silveira

► Lyman- $\alpha$  UV Lamp generates chemical reactions in glycine. ►  $^{252}\text{Cf}$  fission fragments impact on target sample and induce desorption. ► Ion desorption yield measurement gives the abundance of intact molecules in surface. ► Dependence of glycine abundance on irradiation dose is exponential.

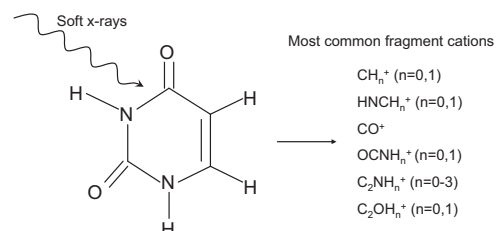


## 82–90

**Fragmentation patterns of core ionized uracil**

E. Itälä, D.T. Ha, K. Kooser, E. Nõmmiste, U. Joost, E. Kukk

► Fragmentation processes are explained by plain bond cleavages of the pyrimidine ring. ► All pyrimidine derivatives fragment essentially the same way. ► The functional groups can have significant effect on fragment abundances.



**Short communication****91–94****Loss of  $\text{Ag}_3$  moiety from clusters  $\text{Ag}_n^+$  ( $n = 4, 6, 8, 10, 12$ ) upon collision induced dissociation**

Rafał Frański, Błażej Gierczyk, Tomasz Kozik

► The  $\text{Ag}_n^+$  ions were generated in the gas phase, by using LDI technique, from  $\text{Ag}(\text{acac})$ .  
► CID MS/MS spectra of the  $\text{Ag}_n^+$  ions were performed. ► Ions  $\text{Ag}_4^+$ ,  $\text{Ag}_6^+$ ,  $\text{Ag}_8^+$ ,  $\text{Ag}_{10}^+$ ,  $\text{Ag}_{12}^+$  loose  $\text{Ag}_3$  moiety (trimer evaporation). ► This result was not observed upon previous studies devoted to the  $\text{Ag}_n^+$  ions.

